DTIC FILE COPY

(2)

AD-A222 391

DTIC ELECTE MAY 23 1990 S B D

DOCUMENTATION PAGE

Form Approved OMB No. 0704-0188

1b RESTRICTIVE MARKINGS

2a SECURITY CLASSIFICATION AUTHORITY

3 DISTRIBUTION/AVAILABILITY OF REPORT
This document has been approved for public release and sale; its distribution is unlimited.

2b DECLASSIFICATION/DOWNGRADING SCHEDULE

4 PERFORMING ORGANIZATION REPORT NUMBER(S)
IBM Research Report RJ7624

5 MONITORING ORGANIZATION REPORT NUMBER(S)
Technical Report #25

6a NAME OF PERFORMING ORGANIZATION
IBM Research Division
Almaden Research Center

6b OFFICE SYMBOL (If applicable)

7a NAME OF MONITORING ORGANIZATION
Office of Naval Research

6c ADDRESS (City, State, and ZIP Code)
650 Harry Road
San Jose, CA 95120-6099

7b ADDRESS (City, State, and ZIP Code)
Chemistry Division Code 1113
Arlington, VA 22217

8a NAME OF FUNDING/SPONSORING ORGANIZATION
Office of Naval Research

8b OFFICE SYMBOL (If applicable)

9 PROCUREMENT INSTRUMENT IDENTIFICATION NUMBER
N00014-84-C-0708, 4131022

8c ADDRESS (City, State, and ZIP Code)
Chemistry Division, Code 1113
Arlington, VA 22217

10 SOURCE OF FUNDING NUMBERS

PROGRAM ELEMENT NO	PROJECT NO	TASK NO	WORK UNIT ACCESSION NO

11 TITLE (Include Security Classification)
Ultrasensitive Laser Spectroscopy in Solids: Statistical Fine Structure and Single-Molecule Detection

12 PERSONAL AUTHOR(S)
W.E. Moerner

13a TYPE OF REPORT	13b TIME COVERED	14 DATE OF REPORT (Year, Month, Day)	15 PAGE COUNT
interim technical	FROM _____ TO _____	1990 March 28	35

16 SUPPLEMENTARY NOTATION
Submitted for publication in The New Journal of Chemistry

17 COSATI CODES		
FIELD	GROUP	SUB-GROUP

18 SUBJECT TERMS (Continue on reverse if necessary and identify by block number)
Statistical Fine Structure, Atomic Properties, Single Molecule Detection, Molecular Properties, Laser Spectroscopy of Solids, Instrumentation, Pentacene in p-terphenyl, ORGANIC COMPOUNDS, Near Field

19 ABSTRACT (Continue on reverse if necessary and identify by block number)

Detailed studies of the low-temperature inhomogeneously broadened 0-0 S_1-S_0 electronic transition of pentacene dopant molecules in p-terphenyl crystals have produced two novel observations which open up a new regime for ultrasensitive laser spectroscopy in solids. The first result, direct detection of intrinsic static absorption fine structure on a MHz scale, called statistical fine structure, arises from number fluctuations in the spectral density of absorbers which scale as the square root of the number of absorbers per homogeneous width. Surprisingly, this effect provides a new method for determining the homogeneous width that does not rely on hole-burning or coherent transients. The second recent observation, detection of the optical absorption of a single pentacene molecule in a p-terphenyl crystal, opens the door to new studies of single, local environments in solids as well as to studies of the interactions of a single absorber with

Cont on Next page

20 DISTRIBUTION/AVAILABILITY OF ABSTRACT
☒ UNCLASSIFIED/UNLIMITED ☐ SAME AS RPT ☐ DTIC USERS

21 ABSTRACT SECURITY CLASSIFICATION
UNCLASSIFIED

22a NAME OF RESPONSIBLE INDIVIDUAL
Dr. W.E. Moerner

22b TELEPHONE (Include Area Code)
(408) 927-2426

22c OFFICE SYMBOL

DD Form 1473, JUN 86 — Previous editions are obsolete — S/N 0102-LF-014-6603

SECURITY CLASSIFICATION OF THIS PAGE
UNCLASSIFIED

megaHertz

external perturbations in which no averaging is performed over large numbers of nominally equivalent local configurations. Both achievements utilized high sensitivity variations of laser frequency modulation spectroscopy to perform the measurement.

Continue
Form 1473, Block 18
Keywords.

OFFICE OF NAVAL RESEARCH

Contract N00014-84-C-0708

R&T Code 4131022

Technical Report No. 25

Ultrasensitive Laser Spectroscopy in Solids: Statistical Fine Structure and Single-Molecule Detection

by

W. E. Moerner

Prepared for Publication

in

The New Journal of Chemistry

IBM Research Division
Almaden Research Center
650 Harry Road
San Jose, California 95120-6099

March 28, 1990

ULTRASENSITIVE LASER SPECTROSCOPY IN SOLIDS: STATISTICAL FINE STRUCTURE AND SINGLE-MOLECULE DETECTION

W. E. MOERNER

IBM Research Division, Almaden Research Center, San Jose, CA 95120 USA

Abstract: Detailed studies of the low-temperature inhomogeneously broadened 0-0 $S_1 \leftarrow S_0$ electronic transition of pentacene dopant molecules in *p*-terphenyl crystals have produced two novel observations which open up a new regime for ultrasensitive laser spectroscopy in solids. The first result, direct detection of intrinsic static absorption fine structure on a MHz scale, called statistical fine structure, arises from number fluctuations in the spectral density of absorbers which scale as the square root of the number of absorbers per homogeneous width. Surprisingly, this effect provides a new method for determining the homogenous width that does not rely on hole-burning or coherent transients. The second recent observation, detection of the optical absorption of a single pentacene molecule in a *p*-terphenyl crystal, opens the door to new studies of single local environments in solids as well as to studies of the interactions of a single absorber with external perturbations in which no averaging is performed over large numbers of nominally equivalent local configurations. Both achievements utilized high sensitivity variations of laser frequency modulation spectroscopy to perform the measurement.

I. INTRODUCTION

Recent progress in the optical detection and spectroscopy of single ions in vacuum confined in electromagnetic traps has led to novel measurements that test our understanding of quantum physics. For example, various workers have achieved direct measurement of quantum jumps, Doppler sidebands, and other fundamental phenomena such as ion crystallization [1,2]. By using laser-induced fluorescence and a novel hydrodynamically-focused flow to confine the molecules and reduce the scattering volume, single molecules of the protein B-phycoerythrin with the equivalent of 25 rhodamine 6G chromophores have also been detected [3,4]. These spectroscopic achievements represent one type of non-invasive measurement that can be performed with a far-field technique like optical spectroscopy. The absorbing center must be confined in a trap or in a flow and background fluorescence signals must be highly controlled to allow such observations.

At the opposite extreme, recent advances with various near-field spectroscopies such as scanning tunnelling microscopy (STM)[5] have provided images of single molecules of benzene and CO on Rh surfaces [6] and images of liquid crystal molecules on graphite [7] to name a few examples. The invention of the STM earned Binnig and Rohrer [5] the Nobel Prize in 1986, and many workers around the world are applying this technique to a large variety of systems. Moreover, the STM work has inspired a new group of surface imaging devices that use a broad variety of interactions for detection[8]. Characteristic of STM studies is the need for a strong bond between the molecule of interest and the underlying surface so that the molecule can remain in a fixed configuration long enough for the tunneling spectrum to be obtained.

It is natural to inquire about the possibility of single-center spectroscopy when the center of interest is a molecular defect hidden deep inside a solid. The detection and spectroscopy of a single absorber in a solid (called in the case of a molecular impurity single-molecule detection, or SMD) would provide a useful

tool for the study of local host-absorber interactions where the absorbing center is essentially at rest, confined by the host lattice, and where the normal averaging over many "equivalent" centers is removed. This paper describes the recent research on the fundamental properties of inhomogeneous lines which has resulted in SMD for the case of a pentacene molecule in Bridgman-grown *p*-terphenyl crystals as a model system[9]. Although this paper focuses on molecular impurity centers, the physical concepts apply equally well to ions, color centers, and other defect absorptions in solids.

As an important first step toward SMD, it was necessary to begin by taking a very detailed look at the inhomogeneously broadened optical absorption line of a defect in a solid with large numbers of absorbers. In this regime, an unusual effect called statistical fine structure (SFS) was observed for the first time [10,11]. SFS results from (static) number fluctuations in the spectral density of absorbers with optical wavelength, and therefore scales as the square root of the number of absorbers in resonance. The observations of SFS and examples of its utility will be described in Section II of this paper. Central to these measurements was the use of a powerful zero-background laser technique called frequency modulation spectroscopy (FMS), first described by Bjorklund[12] in 1980.

With a firm understanding of SFS in inhomogeneous lines, it became possible to approach the ultimate limit of single center detection and spectroscopy, SMD. One motivation for this comes from the fact that for an inhomogeneously broadened line, the various centers located within a homogeneous width of a given laser frequency are located at that particular spectral position for a variety of possible reasons in general. This intrinsic multi-dimensional inhomogeneity cannot be removed with spectral hole-burning or coherent transient techniques. However, with SMD the absorption spectrum of an individual absorber can become directly accessible, as long as no other centers are present at the same frequency. This is a primary reason to pursue the spectroscopy of individual centers in condensed matter. Other motivations

come from the fact that a single molecular impurity is a truly local probe of the minute details of a single local environment in a solid. The use of powerful spectroscopic methods as well as the properties of the inhomogeneous line itself make SMD feasible, and our successful SMD experiments [9, 13, 14] will be described in Section III. With these observations, a new regime of optical spectroscopy may be envisioned in which some of the scientific advances and observations of physical effects made possible by the ion trap and STM techniques may be attempted in condensed matter.

II. STATISTICAL FINE STRUCTURE IN INHOMOGENEOUS LINES

A. The Inhomogeneous Optical Absorption Line in Solids

Generally, absorbing guest centers in solids with zero-phonon transitions form inhomogeneously broadened lines, [15] where the overall line profile is caused by a (usually Gaussian) distribution of center frequencies for the individual absorbers that is broader than the (usually Lorentzian) homogeneous lineshape of the individual absorbers (See Figure 1, left side). The distribution of center frequencies is caused by dislocations, point defects, or random internal electric and strain fields and field gradients in the host material. Inhomogeneous broadening is not only a universal feature of high-resolution laser spectroscopy of defects in solids[16], but it also appears in a fundamental way in other spectroscopies of impurity centers such as NMR, ESR, and Mössbauer absorption. Inhomogeneous broadening also occurs in amorphous hosts, where the center frequency distribution is caused by the large multiplicity of local environments. Although this paper will focus mainly on the lowest electronic transition of the absorbing molecule, all of the concepts apply equally well to inhomogeneously broadened vibronic lines as well as to inhomogeneously broadened purely vibrational zero-phonon lines.

Strong inhomogeneous broadening generally requires low temperatures, because the homogeneous zero-phonon lines become much narrower than the inhomogeneous distribution of center frequencies only when the host phonons are quenched. For example, for pentacene in *p*-terphenyl, the homogeneous width of the lowest electronic transition at 593 nm is 7.8 MHz at 1.5K, [17] while the overall inhomogeneous line is 42 GHz in width [18]. In the single-molecule spectroscopy to be described in Section III, inhomogeneous broadening will be used to select one single absorber for spectroscopy by proceeding out into the wings of the inhomogeneous line as shown on the right side of Fig. 1.[19] Since the center frequencies for these absorbers are displaced very far from the most common center frequencies near the center of the inhomogeneous line, such absorbers have highly unique and improbable strained sites. For the SFS measurements, however, we restrict our attention to the region near the center of the inhomogeneous line.

B. Scaling Properties of SFS

Due to the randomness associated with the imperfections in solid hosts, inhomogeneous absorption lines (at least near their centers) are often approximated by smooth, Gaussian profiles [15,18]. However, since the inhomogeneous line on a microscopic scale is simply a superposition of *discrete* homogeneous lines with widths as much as 1000 times narrower than the overall inhomogeneous profile, the true shape of the inhomogeneous line cannot be a smooth function in reality. In fact, unavoidable number fluctuations in the density of absorbers per unit wavelength interval should give rise to a "spectral noise" on the overall Gaussian background that scales as the square root of the mean number of centers in resonance. To be precise, defining the average number of centers in the probed volume within one homogeneous width of the laser wavelength as $\bar{N}_H$, there should be a statistical fine structure (SFS) present on the absorption profile scaling in absolute magnitude as $\sqrt{\bar{N}_H}$ (in the limit of

$\bar{N}_H >> 1$). Since SFS arises from the absorption of many overlapping impurity absorptions, the absolute magnitude of the SFS is clearly larger than a single-molecule absorption signal (where $\bar{N}_H \simeq 1$). Therefore, observations of SFS would be expected to precede true single-molecule or single-center detection.

A computer simulation of the inhomogeneous lineshape for varying numbers of centers helps in understanding the influence of concentration and sample configuration on the expected size of the SFS signals. We consider a fixed frequency interval $\Delta\nu$ within the inhomogeneous line that satisfies $\Gamma \gg \Delta\nu \gg \gamma$, where γ is the homogeneous linewidth (full width at half-maximum absorption, or FWHM) and Γ is the FWHM of the inhomogeneous line. We define the spectral density of absorbers in the probed volume $g(\nu)$ by requiring that $g(\nu)d\nu$ be the number of absorbers with center frequencies in $d\nu$ at ν. Then the number of centers per homogeneous linewidth is $N_H \equiv \int g(\nu)d\nu$ where the integral is performed over the spectral range γ, and the variations in $g(\nu)$ and thus in N_H with frequency form the underlying source of SFS. Let ΔN_H , $\bar{N}_H$ and $\Delta\alpha$, $\bar{\alpha}$ signify the rms amplitude and mean value of N_H and α, respectively, over $\Delta\nu$.

We make the crucial assumption that the probability of a given center acquiring a particular center frequency in the range $\Delta\nu$ is independent of frequency. This is equivalent to assuming no "microsites" or special frequencies that are more probable than others within the interval. Figure 2 then illustrates by simulation the variations in absorption coefficient that can occur due to statistics alone.

To show how this figure was generated, let $L_\gamma(\nu) = (\gamma/2\pi)/[\nu^2 + (\gamma/2)^2]$ signify the assumed Lorentzian absorption of FWHM γ for each center so that the full inhomogeneous lineshape can be written

$$\alpha(\nu) = s\int_{-\infty}^{+\infty} g(x)L_\gamma(\nu - x)dx \equiv s\, g * L_\gamma(\nu), \qquad (1)$$

where s is the integrated absorption strength per center and the asterisk signifies convolution. Figure 2(a) shows a possible lineshape if only two centers are in $\Delta\nu$, i.e., $\bar{N}_H \simeq 0.2$. Traces 2(b), (c), (d), and (e) show simulated lineshapes for $\bar{N}_H = 1$, 10, 100, and 10^4. Clearly, $\bar{\alpha}$ is growing linearly with $\bar{N}_H$, while the relative fluctuations in absorption $\Delta\alpha/\bar{\alpha}$ are decreasing as $(\bar{N}_H)^{1/2}$. Therefore, in terms of relative changes in absorption it appears that small $\bar{N}_H$ samples ($\bar{N}_H < 10$, for example) might be expected to be optimal for the observation of SFS. However, if fluorescence is used, detecting the small signal from such a small number of centers in the presence of considerable background from the host matrix is quite difficult[20].

Zero-background techniques like FM spectroscopy (see the next section) provide a way around this problem, because the variable measured is $\Delta\alpha$ itself, which is growing as $(\bar{N}_H)^{1/2}$. Trace 2(f), which is a spectrum identical to trace 2(e) with the background removed, demonstrates that SFS is still present even when $\bar{N}_H$ is large. Thus the key to our initial observation of SFS was to measure the *absolute* size of the absorption variations, not the relative size.

C. Laser FM Spectroscopy

Our approach to SFS and SMD for pentacene in *p*-terphenyl avoids the problem of fluorescence backgrounds by using a powerful absorption technique, laser FM spectroscopy (FMS)[12]. The basic operation of FMS is illustrated in the upper part of Figure 3. A tunable single-frequency cw laser beam at optical carrier frequency ω_c is passed through an electro-optic phase modulator to produce light that is frequency-modulated at a rf frequency ω_m in the MHz range. This FM light beam has the spectrum shown in the upper center of the figure: a carrier at the original frequency, plus two sidebands displaced by $\pm\omega_m$ from the carrier. (FMS is often performed in the low-modulation-index regime where higher-order sidebands can be neglected.) If this FM light beam were sent directly to a high-speed photodiode detector (which measures the envelope of the

power absorbed), no photocurrent at ω_m would be detected. In other words, an FM light beam has no amplitude modulation (AM). In the frequency domain, this lack of AM can be understood by noting that one of the two sidebands is in phase and the other out of phase with respect to the carrier. Therefore, the beat signals caused by each sideband interfering with the carrier cancel.

When a spectral feature is present that disturbs the balance between the two sidebands, a rf photocurrent appears that is proportional to the difference in optical absorption at the upper and lower sidebands. This photocurrent at ω_m may be detected (phase-sensitively) by a rf lock-in composed of a mixer driven with a local oscillator derived from the original rf source. The low-frequency or baseband signal at the IF port of the mixer becomes the standard FMS signal, with the following properties[21]: (1) it appears on a background that is derived from the laser noise at ω_m, which may be at the quantum limit if no excess noise is introduced by the detector, (2) the size of the signal is largest when the spectral feature has width comparable to or less than ω_m, and (3) for wide spectral features the FMS signal is proportional to the derivative of the feature with an amplitude approaching zero for increasing width of the feature. Point (1) is responsible for the quantum-limited performance of FM spectroscopy that has been achieved with simple (non-avalanche) photodiodes[22]. Points (2) and (3) are particularly important for detection of weak spectral features, because any undesired optical absorption from other impurities or from the host that is broad compared to ω_m is not detected with appreciable amplitude. With our values of $\omega_m/2\pi = \nu_m = 50 - 150$ MHz, only rigid molecules like pentacene with homogeneous widths less than $\simeq$ 150 MHz will be detected.

More precisely, the crucial feature of the FM technique is that the detected signal varying as $\cos(2\pi\nu_m t)$, $F_1(\nu)$, is proportional to

$$F_1(\nu) \sim -MP_0 e^{-\bar{\alpha}\ell}[\alpha(\nu+\nu_m) - \alpha(\nu-\nu_m)]\ell, \qquad (2)$$

where ν is the laser frequency, ν_m is the rf modulation frequency, P_0 is the laser power on the sample, M is the modulation index, ℓ is the sample length, and $\bar{\alpha}$ is the background value of α. Thus the FM signal measures the difference in $\alpha\ell$ at the two sideband frequencies. (The component of the photocurrent varying as $\sin(2\pi\nu_m t)$, called $F_2(\nu)$, measures a linear combination of the optical dispersion at the carrier and the two sidebands [11].)

The FM signal $F_1(\nu)$ has two well-defined limits depending upon the ratio of ν_m to the linewidth of the spectral features[12]. Let us assume for the moment that the spectral feature of interest is a single Lorentzian of with γ. When $\nu_m \ll \gamma$, $F_1(\nu)$ approaches the derivative of the Lorentzian. When $\nu_m \gg \gamma$, $F_1(\nu)$ consists of two replicas of the Lorentzian line, one positive and one negative, separated by $2\nu_m$. In this regime $F_1(\nu)$ is maximal and independent of ν_m, and it is this regime that we use most often to detect SFS and SMD. Using the scaling results of the last section, the F_1 signal for SFS is proportional to (as long as the optical density is not too large)

$$(\Delta\alpha)\ell = \sigma(\bar{N}_H)^{1/2}/A = \sigma(\rho_H \ell/A)^{1/2}, \tag{3}$$

where σ is the peak absorption cross section, A is the beam area, and the volume density per homogeneous linewidth is $\rho_H = \bar{N}_H/A\ell$. Therefore, $F_1(\nu)$ increases if the concentration of absorbers or the sample length increases, and increases for smaller laser spots. Further, centers with higher cross section lead to larger FM signals.

D. Examples of SFS Spectra

In this section, examples of SFS spectra [11] for the model system composed of pentacene substitutional impurities in *p*-terphenyl crystals at 1.5K will be presented. The pentacene molecules can substitute for any one of the four *p*-terphenyl molecules in the low-temperature unit cell[18], giving rise to four $S_1 \leftarrow S_0$ 0-0 optical absorption origins near 593 nm. named O_1, O_2, O_3, and O_4. We

focus on the inhomogeneously broadened origins O_1 and O_2, because the homogeneous linewidths are smaller here than for the other origins. The spectra were acquired by repetitively scanning a R6G single-frequency dye laser (2.8 MHz linewidth) over the desired frequency range and averaging 64 scans. Unless stated otherwise, the laser was focused to a 20 μm diameter spot, the laser power was 3 μW, and the sample was immersed in superfluid helium at 1.4 K.

An example of the static nature (and repeatability) of the SFS spectra is shown in Figure 4, where the bottom panel shows a 5 GHz wide scan of the SFS near the peak of the O_1 line. Contrary to what the reader might think, this is not a recording of of some noisy signal. The many peaks and valleys are actual, repeatable fine structure as is demonstrated by the two expanded traces in the top panel of Figure 4, the lower of which is an expansion of the trace in the bottom panel and the upper of which is a subsequent acquisition of the same spectral region more than 20 min later. The agreement is quite good, indicating that at 1.4 K there is little or no rearrangement or annealing of the strains and other imperfections in the *p*-terphenyl crystal that were originally "frozen" when the crystal was cooled. Most, if not all, of the slight differences between the spectra are due to the quantum and avalanche noise of the detection system. The bumps and valleys in this figure may be regarded as the "fuzz" on the top of the "haystack" represented by the pentacene inhomogeneous line that results from the statistics of independent, additive random variables.

More insight into the source of SFS can be derived from spectra from different probe volumes. One quickly realizes that since the formation of a specific $g(\nu)$ for a given probe volume is a random process and therefore is a sample of the underlying probability distribution for center frequencies, the SFS spectral structure should change for different probe volumes. Thus an "SFS landscape" of the inhomogeneous line can be generated by acquiring multiple SFS spectra as a function of laser spot position, as in Figure 5. This 3-dimensional plot covers a 200 MHz range in frequency and a 200 μm range in

laser spot position. Such a display allows one to search for "microsites", i.e., special (more probable) frequencies that would appear to be ridges in this 3-dimensional plot. No evidence for microsites or departures from the statistical source for SFS have been observed in this system. In particular, as one would expect from the number fluctuation source for SFS, the rms amplitude of the SFS spectra should grow as $(\bar{N}_H)^{1/2}$, and a measured dependence of $(\bar{N}_H)^{0.54\pm0.05}$ has been observed experimentally[10].

The measurement of SFS provides a new window on inhomogeneously broadened lines with intrinsic detail and complexity. For example, recording of SFS spectra over a larger fraction of the inhomogeneous profile may provide new information about the distribution of optical absorption energies available to the impurity centers. For example, it should be possible to detect the crossover regime where the rms value of the SFS spectra changes from $\sqrt{\bar{N}_H}$ scaling to $\bar{N}_H$ scaling. In addition, the presence of well-defined external perturbations such as Stark, Zeeman, or stress splittings can be detected by cross-correlation of SFS spectra with and without the external perturbation present. Temperature dependent cross-correlation experiments would allow determination of the temperature at which strain annealing of the spectral density $g(\nu)$ occurs.

D. Determination of Homogeneous Width

Because the inhomogeneous line is a simple linear superposition of individual Lorentzian profiles for the various centers in the probe volume (as long as the centers may be regarded as isolated), estimates of the underlying value of γ can be extracted from the spectra by exploiting the properties of autocorrelation functions[11]. We consider the expected autocorrelation of the F_1 spectra, $<F_1 \star F_1>(\nu)$, in the limit $\nu_m \gg \gamma$. The result is

$$<F_1 \star F_1>(\nu) \propto -L_{2\gamma}(\nu + 2\nu_m) + 2L_{2\gamma}(\nu) - L_{2\gamma}(\nu - 2\nu_m). \qquad (4)$$

At the origin ($\nu = 0$), the expectation value of the autocorrelation of the FM signal has a FWHM equal to twice that for the underlying homogeneous absorption lines. Thus an estimate for γ can be derived from the FWHM or, better, the second derivative of $< F_1 \bigstar F_1 > (\nu)$ at the origin:

$$\gamma \simeq \left[\frac{-2 < F_1 \bigstar F_1 > (0)}{< F_1 \bigstar F_1 > ''(0)} \right]^{1/2} . \qquad (5)$$

where the double prime signifies second derivative. (Eqn. (5) is also true[11] for $< F_2 \bigstar F_2 >$.)

To show experimentally how the expectation of the autocorrelation of the SFS signals approaches Eqn. (4), Figure 6 shows examples of measured single autocorrelation functions as well as the average of 10 autocorrelations for both F_1 and F_2. In order to obtain the best estimate of the autocorrelation function near the origin, long (4.8 GHz) laser scans should be used. For a single crystal sample with concentration 3×10^{-7} moles/mole, Eqn. (5) yields $\gamma = 7.9 \pm 0.8$ MHz for the O_1 site at 1.4 K by analyzing the autocorrelations of six SFS spectra over a 4.8 GHz spectral range using $\nu_m = 150$ MHz. This value is consistent with the previously reported value[17] of 7.8 ± 0.6 MHz obtained using coherent transient techniques.

While this method of obtaining the homogeneous width worked well for pentacene in *p*-terphenyl, one must realize that the autocorrelation of SFS spectra is not a reliable measure of γ in all materials. For example, if spectral hole-burning is strong or if spectral diffusion causes the center frequency of absorption for the various centers to change rapidly, the SFS spectrum will be difficult to acquire. However, in cases with weak hole-burning and weak spectral diffusion, this method of obtaining γ should work as well as other techniques as long as the signal-to-noise ratio of the SFS spectrum is reasonable.

E. Observations of SFS in Other Materials

Subsequent to the first observations of SFS, other researchers utilized both FM and fluorescence to observe SFS in other classes of materials. These experiments moved closer and closer to the goal of single-center spectroscopy by observing SFS at smaller and smaller values of $\bar{N}_H$. Lange et al. [23] relied upon fluorescence excitation of Sm^{2+} ions in CaF_2 at 77K with a fixed frequency laser in tightly focused spots. These researchers saw Poisson fluctuations in the detected fluorescence as a function of the position of the focal spot and concluded that they had reached the level $\bar{N}_H = 5$. A particularly novel approach, developed by the Yen group at the University of Georgia [24,25], used laser fluorescence excitation in a glass fiber doped with Nd^{3+} ions. Here the fiber geometry effectively maintained a small focus and a small probing volume in order to reduce background signals from the host. The measured SFS led these researchers to conclude that they had reached $\bar{N}_H$ values on the order of a few tens of ions. In both of these cases, special detection geometries were required to reduce interfering background fluorescence from Rayleigh and Raman scattering.

Eqn. (3) shows that SFS becomes harder and harder to detect when σ decreases. The drop in signal can be partially offset by increasing the concentration of centers, but for constant optical density the signal still suffers as the square root of the cross section. Nevertheless, FM techniques with the addition of Stark secondary modulation to remove residual AM allowed the observation of SFS for Cr^{3+} ions in alexandrite[26]. Another approach for low σ is to maintain a focused spot over a long distance in an optical fiber[11]. In this case the SFS signal increases as the square root of the fiber length, as long as the optical density is less than unity. Using this fact and FM spectroscopy techniques, Brocklesby et al. [27] have observed SFS for Nd^{3+} ions in a silica fiber. These experiments demonstrate that SFS can indeed be detected for absorbers in amorphous hosts and for relatively weakly absorbing centers. The generality of SFS in other systems is a matter of detectability in each individual case.

III. SINGLE MOLECULE DETECTION

A. Detection Challenges and Experimental Approach

Compared to the previous single-absorber experiments on ions in traps, molecules in hydrodynamic flows, and molecules on surfaces, SMD in solids provides a different set of experimental challenges. The problem can be likened to finding a needle in a haystack, because unlike the ion-trap experiments, for example, the molecule of interest is hidden within a solid containing a large number ($\simeq 10^{12} - 10^{18}$) of "non-absorbing", potentially interfering host molecules within the laser focal volume. If laser-induced fluorescence excitation were used for SMD and the host molecules had appreciable Raman (or Rayleigh) scattering cross sections, the signal from the one absorbing molecule could be swamped by the scattering signal from the host. Unlike the hydrodynamic focusing experiments, it is not always possible to reduce the host scattering volume. Furthermore, it would be intriguing to measure the absorption spectrum of a single absorber instead of simply detecting its presence in a digital fashion at a fixed laser wavelength.

Rather than utilizing fluorescence excitation methods where the chief experimental problem is the reduction of interfering scattering signals, we have chosen an alternative route to SMD, namely, laser FM spectroscopy[12] as described above with one important added improvement, double modulation with either electric fields or stress fields to remove residual amplitude modulation. FM spectroscopy also has the advantage that it is sensitive only to spectral features with widths on the order of the modulation frequency ν_m. Therefore, any impurity molecules in the host matrix with wide absorption lines as a result of stronger electron-phonon coupling or much shorter excited state lifetimes than that for pentacene are not observed.

The size of the expected absorption signal from a single molecule is straightforward to estimate[9]. The change in absorbance when only one sideband

passes through the feature, $(\Delta\alpha)L$, is given by the probability of absorption of a photon in the incident beam by the molecule, σ/A, where σ is the peak absorption cross section and A is the area of the laser beam. Clearly, then, one would prefer tightly focused laser spots and molecules with strong absorptions. In our experiment, the focal spot was $\simeq 3$ μm in diameter, and the peak (low-temperature) absorption cross section for pentacene at 1.4 K is 9.3×10^{-12} cm^2, yielding an absorbance change of $\simeq 10^{-4}$. This is not an extremely small signal except that detection must be performed with a light intensity that does not produce extreme power broadening. To meet this constraint in a tightly focused spot, we performed measurements with only 0.1 μW of light at the detector. Even at this level it was necessary to accept some amount of triplet bottleneck power broadening. Another problem with FMS at low light levels is the need to avoid detector Johnson noise. This can be accomplished with the use of an avalanche photodiode detector which has intrinsic gain. However, avalanche photodiodes have an excess multiplicative noise which requires operation somewhat above the quantum limit.

B. Single-Molecule Spectra Using FM/Stark Double Modulation

There is one background signal from FMS that must be avoided to achieve the high sensitivity required for SMD. Since the method directly senses the conversion of FM into AM, any residual AM (also called RAM) from imperfections in the electro-optic modulator can give rise to a spurious background signal. To overcome this, we utilized a secondary modulation of the spectral feature itself. Figure 7 shows a schematic of the apparatus for the case where the secondary modulation was produced by an electric field oscillating at a relatively low frequency f in the kilohertz range. The electric field shifts the absorption profile twice each cycle via the quadratic Stark effect. The FM part of the detection system operates as described above. The effect of the secondary modulation is to produce amplitude modulation of the light beam at $\nu_m \pm 2f$ whenever a narrow

optical absorption interacts with the optical sidebands. The photocurrent is first demodulated by a mixer M driven at ν_m, and then the output of the mixer is processed by a final lock-in amplifier LIA at 2f. Because the physical effects giving rise to the RAM are insensitive to the Stark modulating field, this detection system yields a signal that is free from RAM background.

In addition to this FM/Stark technique, we also separately utilized a different secondary modulation to achieve SMD, ultrasonic (stress) modulation, which operates in a similar fashion by shifting the homogeneous line in a periodic fashion (see the next section). It is clear that other local perturbations of the impurity molecule might also be used for double-modulation detection. Alternatively, other RAM suppression methods that do not require secondary modulation could be utilized [28,29].

Figure 8 shows examples of the spectra for the FM/Stark case. The first three traces show simulations to illustrate the expected single-molecule lineshape for either Stark or ultrasonic double modulation. Trace 8(a) shows a Lorentzian absorption profile of width γ, and trace 8(b) shows the expected simple FM signal[21]: two copies of the absorption line with opposite sign, spaced by $2\nu_m = 150$ MHz (in the limit $\gamma << \nu_m$). With secondary modulation that causes frequency shifts less than the linewidth, the resulting double-modulation lineshape is the derivative of the simple FM lineshape (trace 8(c)). Thus the signature of a single molecule is a "W"-shaped feature with a large negative slope and a large positive slope separated by $2\nu_m$.

In a typical experiment, the laser frequency was set near the center of the inhomogeneous line, and the resulting strong SFS signal was used to optimize the optical and electronic configuration. Then as the laser wavelength was moved out into the wings of the line, the SFS amplitude dropped uniformly. Eventually spectra that appear to be superpositions of 2-5 single-molecule spectra like trace 8(c) were observed. Finally, sufficiently far out into the wings of the line, true single-molecule spectra could be recorded. Trace 8(d) shows a set of eight

FM/Stark double modulation spectra of a strong in-focus molecule far out in the long-wavelength edge of O_1, along with several unavoidable weak repeatable features from out-of-focus molecules at the left edge of the laser scan range. These out-of-focus features were caused by molecules not located at the laser waist position (see Fig. 1) and may be suppressed in future experiments with thinner samples. The fiducial bar marks a spectral range equal to $2\nu_m$. Trace 8(e) shows the average of the eight scans in 8(d), along with a fit to the central feature generated by a simple model for the double-modulation process[14]. The fit to the essential features of the SMD lineshape is reasonable, and the homogeneous width required by the fitting process is somewhat larger than the low-power homogeneous width, as expected, due to the small amount of laser power broadening.

Trace 8(f) shows the detected signal from a laser wavelength so far away from the pentacene site origins that no molecules are expected to lie in the laser scan range; this is the background shot and avalanche noise. In samples of undoped pure *p*-terphenyl, only a baseline noise level similar to the off-line data in Fig. 8(f) was observed, even near the center of the inhomogeneous line. Trace 8(g) shows spectra of the strong SFS observed near the center of the inhomogeneous line using a smaller number of averages. This spectrum is composed of a superposition of many "W" profiles like Figure 8(d) with many different center frequencies, illustrating the qualitative difference between spectra of large numbers of molecules (Fig. 8(g)) and spectra of one molecule (Fig. 8(d)).

One problem with the FM/Stark technique is the possibility of charge injection and motion of trapped charges at the relatively high fields ($\simeq$ 40 kV/cm) required to produce appreciable quadratic Stark shifting. Such effects would greatly perturb the local field around the pentacene molecule, making detection of the spectrum difficult. That some amount of charge injection and/or motion can occur was verified in our experiments by the observation of spectral features responding to the linear Stark effect[14]. An interesting possibility for future

experiments would be to measure both the linear and the quadratic Stark effect for the same molecule, from which the true local field could be determined.

C. Single-Molecule Spectra Using FM/Ultrasound

The study of the local surroundings of pentacene molecules with single injected charge carriers nearby may become an interesting field; however, for the detection and spectroscopy of single dye molecules the effect of charge injection and motion is undesirable, since it gives rise to poor reproducibility of the Stark shifts. In order to overcome this problem and to provide confirmation of our single-molecule results with a distinct technique, we used a different secondary modulation of the absorption lines, namely the application of time-varying stress fields with ultrasound. We call this double-modulation detection scheme FM/US, for FM/ultrasound.

The FM/US technique is related in principle to earlier spectral hole detection experiments with ultrasonic waves[30]. The difference here is that in addition to the usual phase-modulation of the light beam and FM detection with a double-balanced mixer at ν_m, the sample was mounted directly on an ultrasonic transducer driven at a different rf frequency ν_A in the range 1-5 MHz. Both transparent transducers and opaque transducers in reflection were utilized. As in the FM/Stark case, the time-varying stress field shifts the single molecule absorption without affecting the unwanted RAM signal. The corresponding secondary demodulation was performed at ν_A using a second rf mixer. Good single-molecule spectra were obtained with both longitudinal and transverse ultrasonic waves, as will be demonstrated below.

The two traces in Fig. 9(a) show SFS spectra taken at the center of the O_1 band (592.321 nm) using secondary modulation with transverse ultrasound at a frequency $\nu_A = 4.9$ MHz. Upon proceeding out in the wings of the inhomogeneous line, the SFS amplitude was observed to decrease until multiple-molecule and then single-molecule spectra were observed. The traces (b) through (e) show

scans over a spectral region at the blue edge of O_2 (592.004 nm). These spectra were recorded using different light modulation frequencies of 91 MHz (b), 76 MHz (c), 61 MHz (d), and 51 MHz (e). Although the signal-to-noise ratio is somewhat worse than the FM/Stark case (partly due to the averaging of only 128 scans for each trace), a "W"-like single-molecule signal is clearly visible in all of these traces. As the FM modulating frequency ν_m is decreased, the "W" lineshape contracts such that the distance between the downward and the upward slope is always equal to $2\nu_m$. The fiducial bars above the traces mark these distances. The fact that a change of ν_m causes a symmetrical contraction or expansion is the final proof that the "W"-like spectral features are really due to single molecules (or several molecules absorbing at exactly the same frequency). If these signals were composed of spectral features arising from several molecules at several wavelengths, they would not change in such a systematic manner. The SFS signal at the line center, for instance, does not exhibit well-defined changes when ν_m is varied. The possibility that the "W"-like line shapes are generated by more than one molecule absorbing at exactly the same wavelength, on the other hand, cannot be totally ruled out, but this seems extremely unlikely so far away from the center of the inhomogeneous line.

The last two pairs of traces in Fig. 9, (f) and (g), are spectra recorded very far away from the pentacene absorption lines (at 590.452 nm) and scans with no light falling on the detector, respectively. The comparison between (f) and (g) shows that the sensitivity of our double-modulation method is limited by light-related noise (f) which is distinctly larger than the background noise of the electronics (g). However, as was mentioned earlier, this measurement is not fully quantum-limited but contains a contribution from the avalanche noise of the detector.

In the case of secondary modulation with transverse ultrasound, the signal-to-noise ratio was worse than that for the FM/Stark technique, probably due to a smaller stress-induced shift of the pentacene absorption. The repeatability

of the spectra was improved, however. More details of the FM/US experiments as well as measurements with longitudinal ultrasound may be found in Reference 14.

IV. CONCLUSION

By utilizing the near-quantum-limited performance and low background of laser FM spectroscopy, the intrinsic fine structure on inhomogeneous lines in solids, statistical fine structure, was detected for the first time. Armed with a detailed understanding of SFS and improvements to FMS to remove RAM, it thus became possible to measure the optical absorption spectrum of a single molecule of pentacene in *p*-terphenyl. That our spectra were indeed single-molecule spectra is supported by the following evidence: the shape of the observed features, the position relative to the pentacene in *p*-terphenyl origins, the lack of such signals in undoped samples, the dependence of the spectra upon FM modulating frequency, and the appearance of single-molecule spectra with both the FM/Stark and FM/US techniques with both transverse and longitudinal ultrasound.

One experimental shortcoming of zero-background techniques is the difficulty in absolute calibration of the observed signals. We attempted to carefully do this by using a FM signal of known amplitude, but the amount by which the absorption lines were shifted by the secondary modulation could only be estimated. In spite of these limitations, the size of the single-molecule signals appears to be somewhat larger than expected given our level of power broadening. This intriguing observation (which needs to be confirmed in future experiments) suggests that pentacene molecules in the highly strained, improbable sites far out in the wings of the inhomogeneous line may have altered intersystem crossing rates. Such effects have been observed before in the case of n-π^* transitions of benzophenone[31]. Another possibility for altered intersystem crossing may be the presence of a nearby heavy atom impurity.

A number of fascinating future experiments may be contemplated based on the single-molecule detection techniques presented here. The molecule absorbs a large number of photons (on the order of 10^8) during the detection process, hence the absorption profile measured is the "time-average" lineshape which by the ergodic theorem must be equivalent to a true ensemble average. However, near the center of the inhomogeneous line all the molecules at a given frequency may not be equivalent members of the same ensemble. Therefore, it would be interesting to measure the true single-molecule linewidth as a function of optical wavelength and temperature using a detection method allowing lower light probing levels. Nonlinear spectroscopy to measure the AC Stark effect for a single isolated molecule may also be performed. With the proper choice of lifetimes, one would expect quantum jumps and other processes observed for single ions in vacuum electromagnetic traps to be observable. The door is then open to photochemical experiments on single absorbers.

The attainment of single-molecule detection and spectroscopy in solids opens up a new frontier of single-absorber experiments in which the measured properties of the absorbing center are not averaged over many "equivalent" absorbers. Here the absorbing entity is exquisitely sensitive to the symmetry and perturbations introduced by the local environment such as the local vibrational modes and the true local fields. While as a general technique the method presented here is not applicable to all molecular impurities, it can be applied to the large number of absorbing ions and molecules in solids that have zero-phonon transitions and reasonable absorption strength. The detectability of the resulting single-center signal, which ultimately depends upon the absorption strength and upon quantum noise limits, must be evaluated in each case. For situations in which the molecular linewidth is large, recent important advances in two-tone FM spectroscopy [32, 33] make FMS practical with very large sideband spacings.

The author acknowledges seminal collaborations with T. P. Carter on the statistical fine structure experiments and with L. Kador on the single-molecule detection studies. This work was supported in part by the U. S. Office of Naval Research.

REFERENCES

1. See for example Itano W. M., Bergquist J. C., Wineland D. J., *Science*, 1987, **237**, 612 and references therein.
2. Diedrich F., Peik E., Chen J. M., Quint W., Walther H., *Phys. Rev. Lett.*, 1987, **59**, 2931.
3. Nguyen D. C., Keller R. A., Jett J. H., Martin J. C., *Anal. Chem.*, 1987, **59**, 2158.
4. Peck K., Stryer L., Glazer A. N., Mathies R. A., *Proc. Nat. Acad. Sci. USA*, 1989, **86**, 4087.
5. Binnig G., Rohrer H., *Rev. Mod. Phys.*, 1987, **59**, 615.
6. Ohtani H., Wilson R. J., Chiang S., Mate C. M., *Phys. Rev. Lett.*, 1988, **60**, 2398.
7. Foster J. S., Frommer J. E., *Nature*, 1988, **333**, 542.
8. Pool R., *Science*, 1990, **247**, 634.
9. Moerner W. E., Kador L., *Phys. Rev. Lett.*, 1989, 62, 2535.
10. Moerner W. E., Carter T. P., *Phys. Rev. Lett.*, 1987, **59**, 2705.
11. Carter T. P., Manavi M., Moerner W. E., *J. Chem. Phys.*, 1988, **89**, 1768.
12. Bjorklund G. C., *Opt. Lett.*, 1980, **5**, 15.
13. Moerner W. E., L. Kador, *Analyt. Chem.*, 1989, **61**, 1217A.
14. Kador L., Horne D. E., Moerner W. E., *J. Phys. Chem.*, 1990, **94**, 1237.
15. Stoneham A. M., *Rev. Mod. Phys.*, 1969, **41**, 82.
16. See Yen W. M., Selzer P. M., eds., "Laser Spectroscopy of Solids", Springer Topics in Applied Physics, Vol. 49, Springer, Berlin, 1981.
17. Patterson F. G., Lee H. W. H., Wilson W. L., Fayer M. D., *Chem. Phys.*, 1984, **84**, 51.
18. Olson R. W., Fayer M. D., *J. Phys. Chem.*, 1980, **84**, 2001.
19. The reader will recognize that it would also be possible to drastically lower the impurity concentration and work near the center of the inhomogeneous

line. We chose the present approach, because by tuning to the center of the inhomogeneous line where N is large, a convenient alignment signal exists that can be used to optimize the detection system. Then, by tuning out into the wings, single molecule absorptions can be observed.

20. For a description of background problems for liquid hosts, see Nguyen D. C., Keller R. A., Trkula M., *J. Opt. Soc. Am. B*, 1987, **4**, 138.
21. Bjorklund G. C., Levenson M. D., Lenth W., Ortiz C., *Appl. Phys. B*, 1983, **32**, 145.
22. Levenson M. D., Moerner W. E., Horne D. E., *Opt. Lett.*, 1983, **8**, 108.
23. Lange R, Grill W., Martienssen W., *Europhys. Lett.*, 1988, **6**, 499.
24. Yen, W. M., *Proc. Soc. Photo-Opt. Instrum. Engr.*, 1988, **1033**, 183.
25. Yen W. M., "Introduction: Advances in Laser Spectroscopy of Solids," Yen W. M. Ed., *"Laser Spectroscopy of Solids II"*, Springer Topics in Applied Physics Vol. 65, Springer, Berlin, Heidelberg, 1989, p. 23.
26. Carter T. P., Horne D. E., Moerner W. E., *Chem. Phys. Lett*, 1988, **151**, 102.
27. Brocklesby W. S., Golding B., Simpson J. R., *Phys. Rev. Lett.*, 1989, **63**, 1833.
28. Gehrtz M., Bjorklund G. C., Whittaker E. A., *J. Opt. Soc. Am. B*, 1985, **2**, 1510.
29. Wong N. C., Hall J. L., *J. Opt. Soc. Am. B*, 1985, **2**, 1527.
30. Moerner W. E., Huston A. L., *Appl. Phys. Lett.*, 1986, **48**, 1181.
31. Jankowiak R., Bässler H., *Chem. Phys. Lett.*, 1984, **108**, 209.
32. Janik G. R., Carlisle C. B., Gallagher T. F., *J. Opt. Soc. Am. B*, 1986, **3**, 1070.
33. Cooper D. E., Carlisle C. B., *Opt. Lett.*, 1988, **13**, 719.

Figure Captions

FIGURE 1. Schematic showing an inhomogeneous line at low temperatures and the principle of single-molecule detection in solids. The lower part of the figure shows how the number of impurity molecules in resonance in the probed volume can be varied by changing the laser wavelength. The laser linewidth ($\simeq$ 3 MHz) is negligible.

FIGURE 2. Simulated absorption spectra with different values of $\overline{N}_H$. Traces (a) through (e) correspond to $\overline{N}_H$ values of 0.2, 1, 10, 100 and 10,000, respectively. Trace (f) is an expanded trace of the same data as in (e).

FIGURE 3. Schematic showing the principle of FM spectroscopy. The upper part of the figure shows the dye laser spectrum before the electro-optic phase modulator (EO), after the EO, and after the sample. The symbols are defined in the text.

FIGURE 4. Wide range scan of SFS. The lower panel shows the result of 64 averages of a 5 GHz scan of the SFS on the O_1 line at 1.4 K. The upper panel shows a portion of the same spectrum on an expanded frequency scale together with another acquisition of the spectrum taken more than twenty minutes later, offset for clarity.

FIGURE 5. SFS structure versus laser spot position and laser frequency near the inhomogeneous line center for pentacene in *p*-terphenyl. A sequence of 100 spectra were obtained, moving the 20μm laser spot by 2μm after each spectrum, and the results plotted as a contour plot of the SFS signal to show the SFS "landscape".

FIGURE 6. Autocorrelations of SFS spectra in F_1 and F_2 for the O_1 site with $\nu_m = 150$ MHz. Traces (a) and (b) show typical normalized autocorrelations of single SFS spectra. Traces (c) and (d) show the appearance of the peaks described by Eqn. (3) and by a similar equation[8] for F_2 obtained by averaging only ten such spectra.

FIGURE 7. Schematic showing the principle of FM/Stark secondary modulation. The upper part of the figure shows the dye laser (DL) spectrum before the electro-optic phase modulator (EO), after the EO, and after the sample in the cryostat C. Legend: rf - rf oscillator at ω_m, APD - avalanche photodiode detector, M - double-balanced mixer, HV - high voltage source, LIA - lock-in amplifier, DS - digital storage and averaging oscilloscope.

FIGURE 8. Single-molecule spectra using the FM/Stark technique (quadratic Stark effect). (a) Simulation of absorption line. (b) Simulation of FM spectrum for (a), $\nu_m = 75$ MHz. (c) Simulation of FM/Stark double-modulation lineshape. (d) SMD spectra at 592.423 nm, 512 averages, 8 traces overlaid, bar shows value of $2\nu_m = 150$ MHz. (O_1 line center is at 592.326 nm .) (e) Average of traces in (d) with fit to the in-focus molecule (smooth curve). (f) Signal very far off line at 597.514 nm, same conditions. (g) Traces of SFS at the O_2 line center, 592.186 nm, 128 averages each. The vertical scale is exact for (d); all the other traces have the same scale but are offset vertically for clarity.

FIGURE 9 FM/US spectra with transverse (shear) ultrasound, 128 averages each. (a) SFS at O_1 line center (592.321 nm) (b) SMD, S_1 phase, $\nu_m = 91$ MHz, 592.004 nm. (c) Same region, $\nu_m = 76$ MHz (d) Same region, $\nu_m = 61$ MHz (e) Same region, $\nu_m = 51$ MHz (f) Far away from the pentacene absorption lines, 590.452 nm. (g) No light on the detector.

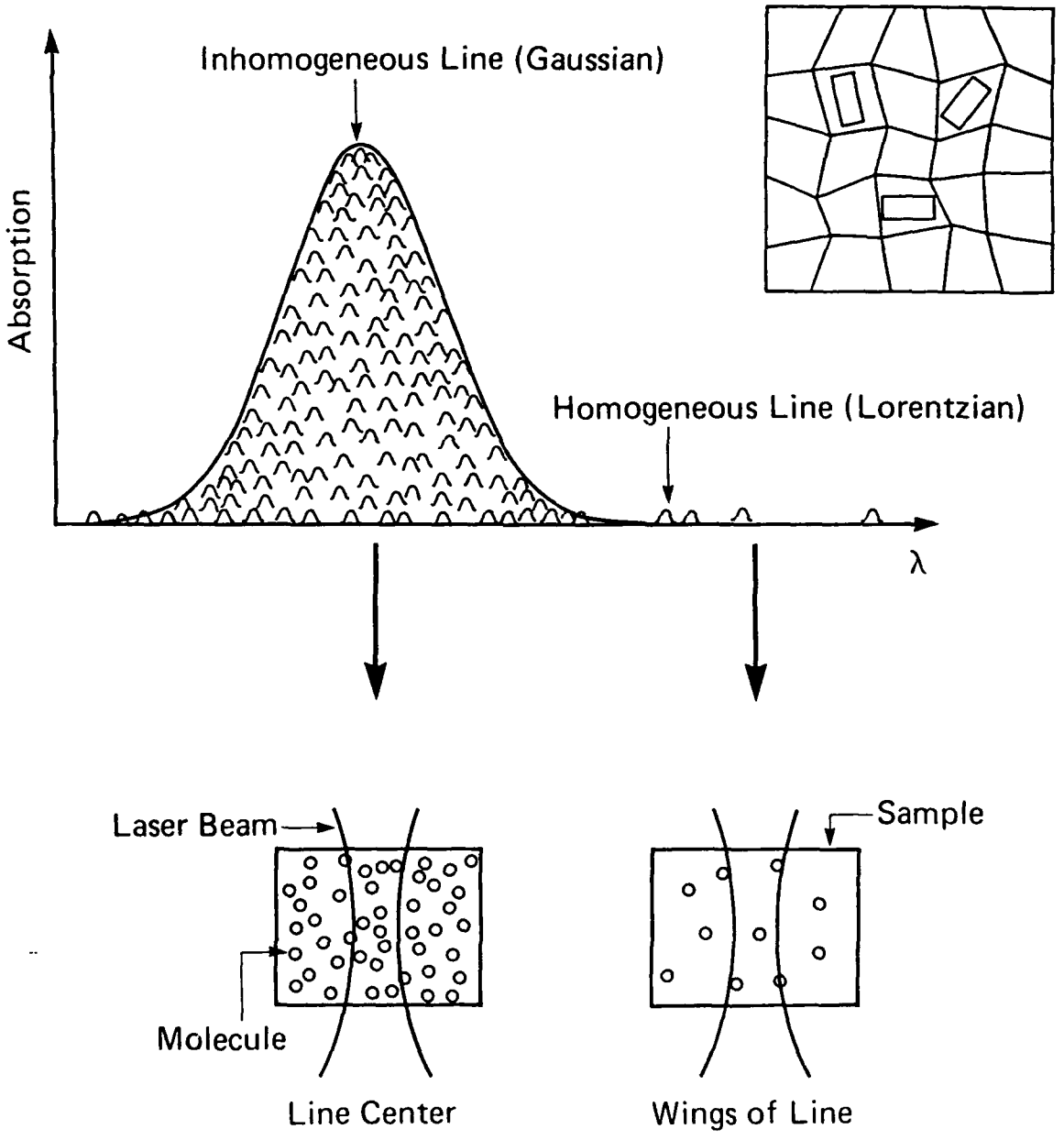
Inhomogeneous Line (Gaussian)
Absorption
Homogeneous Line (Lorentzian)
λ
Laser Beam
Molecule
Line Center
Sample
Wings of Line

Figure 1

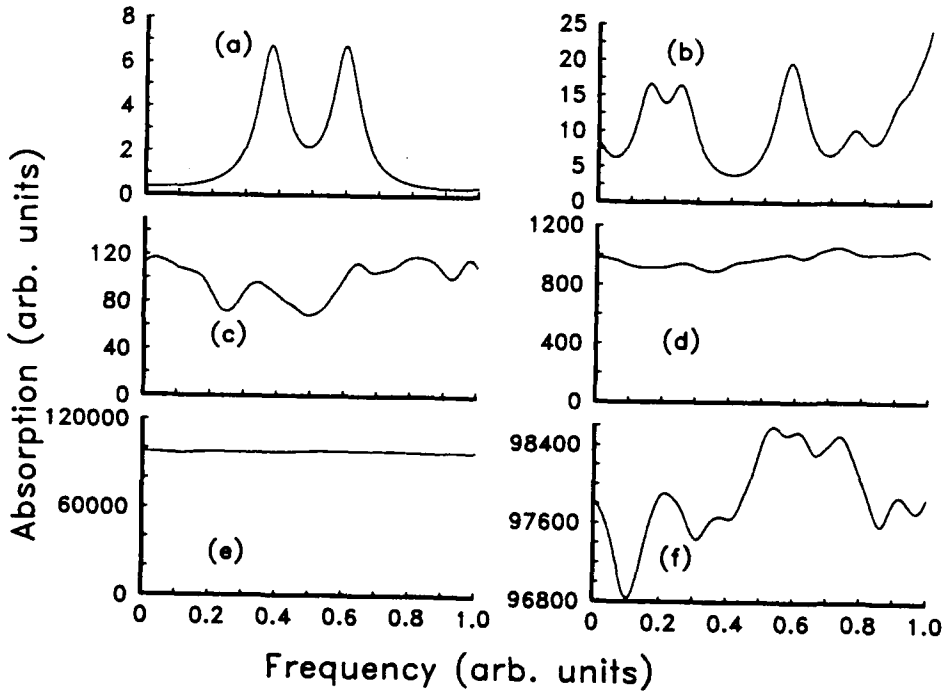

Figure 2

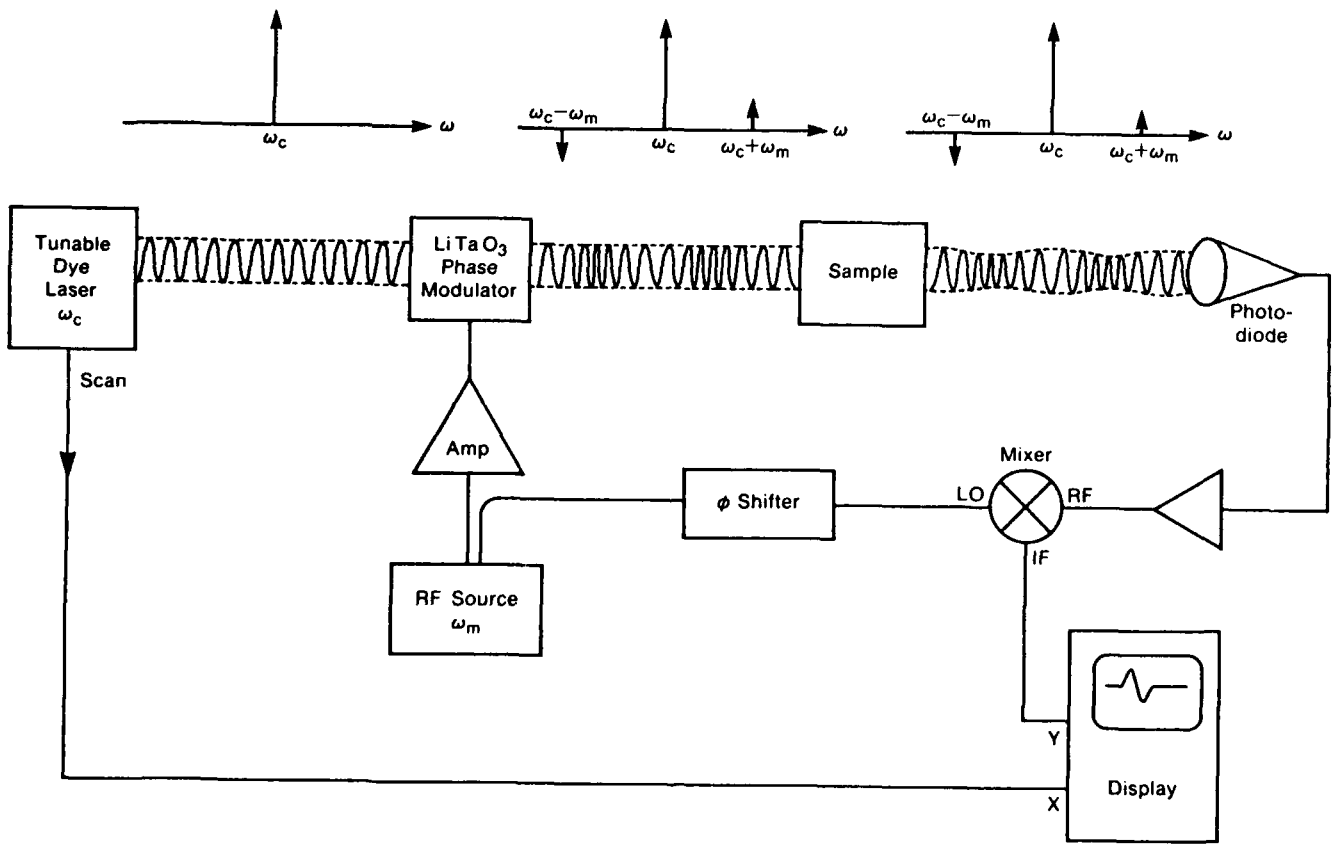
ω_c
ω
$\omega_c-\omega_m$
ω_c
$\omega_c+\omega_m$
ω
$\omega_c-\omega_m$
ω_c
$\omega_c+\omega_m$
ω
Tunable Dye Laser ω_c
Li Ta O_3 Phase Modulator
Sample
Photo-diode
Scan
Amp
Mixer
LO
RF
IF
ϕ Shifter
RF Source ω_m
Y
X
Display

Figure 3

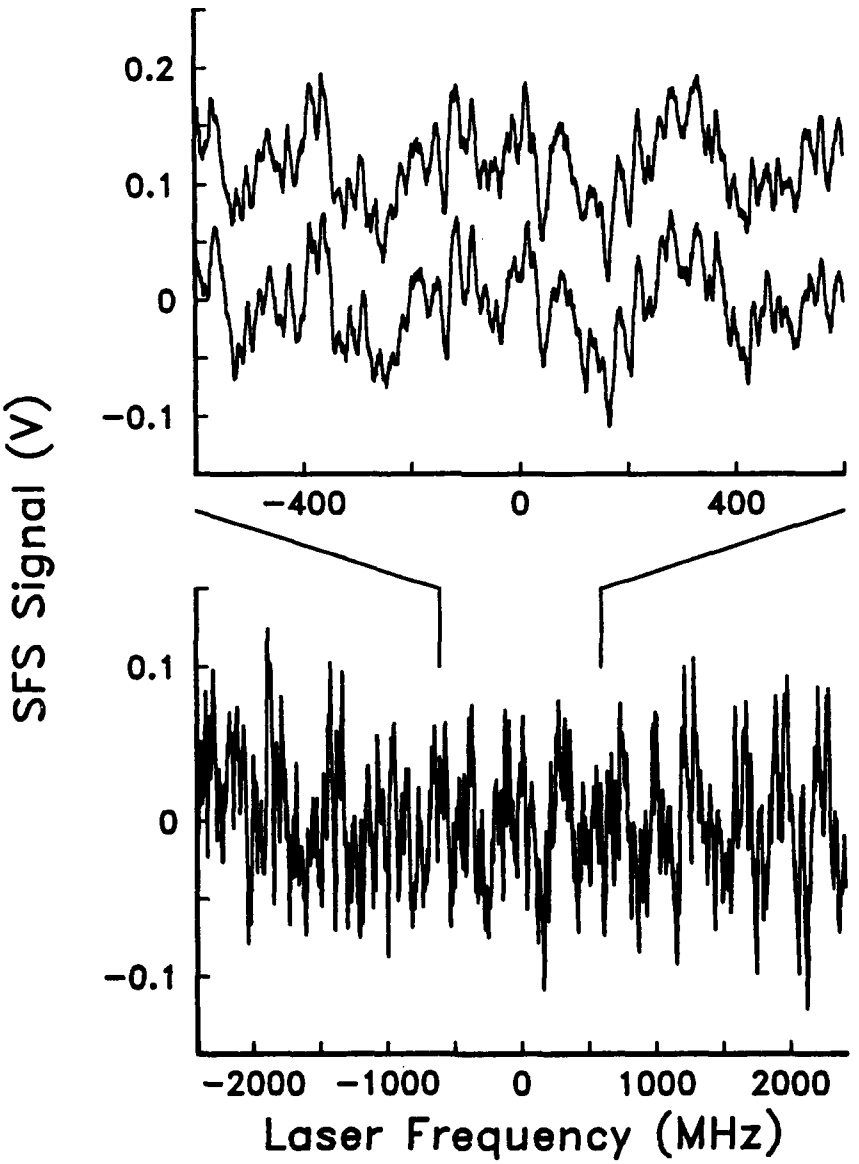
0.2
0.1
0
−0.1
−400
0
400
0.1
0
−0.1
−2000
−1000
0
1000
2000
SFS Signal (V)
Laser Frequency (MHz)

Figure 4

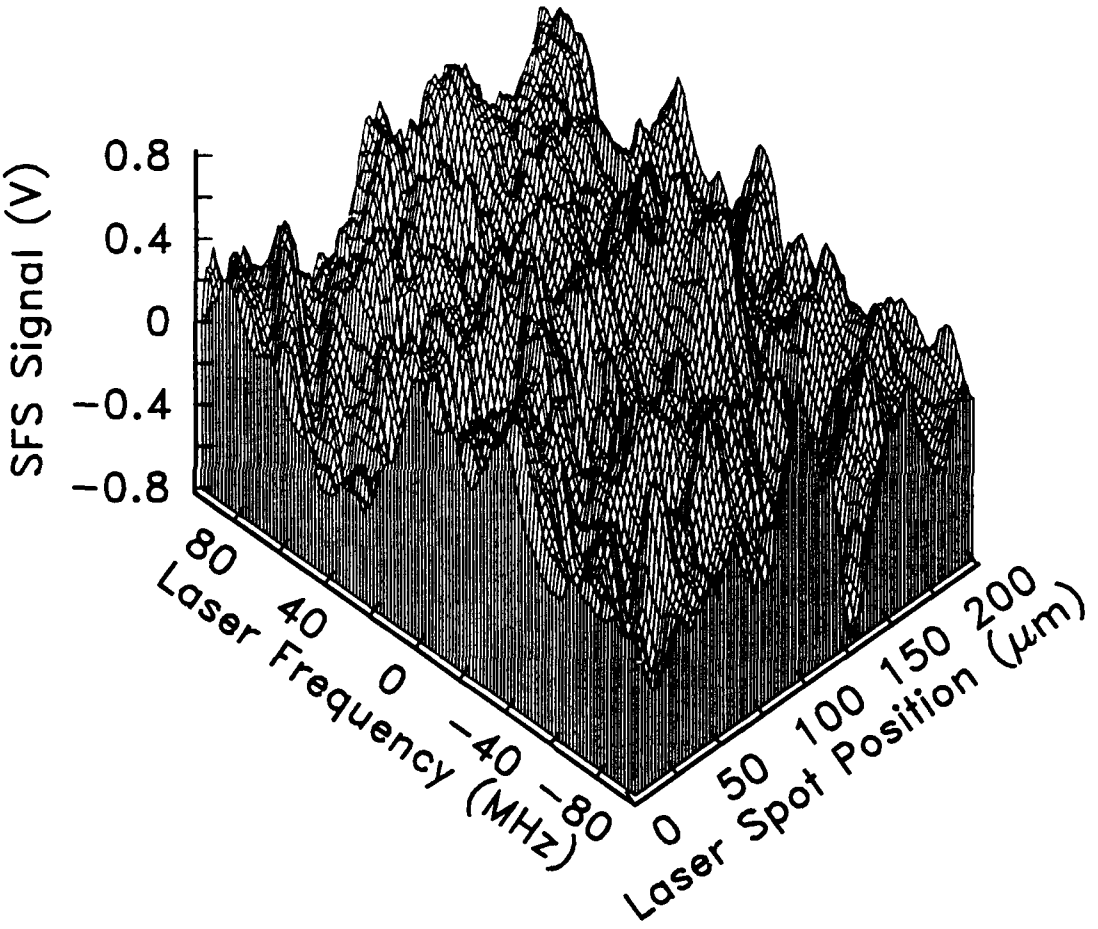
SFS Signal (V)
0.8
0.4
0
−0.4
−0.8
80
40
0
−40
−80
Laser Frequency (MHz)
0
50
100
150
200
Laser Spot Position (μm)

Figure 5

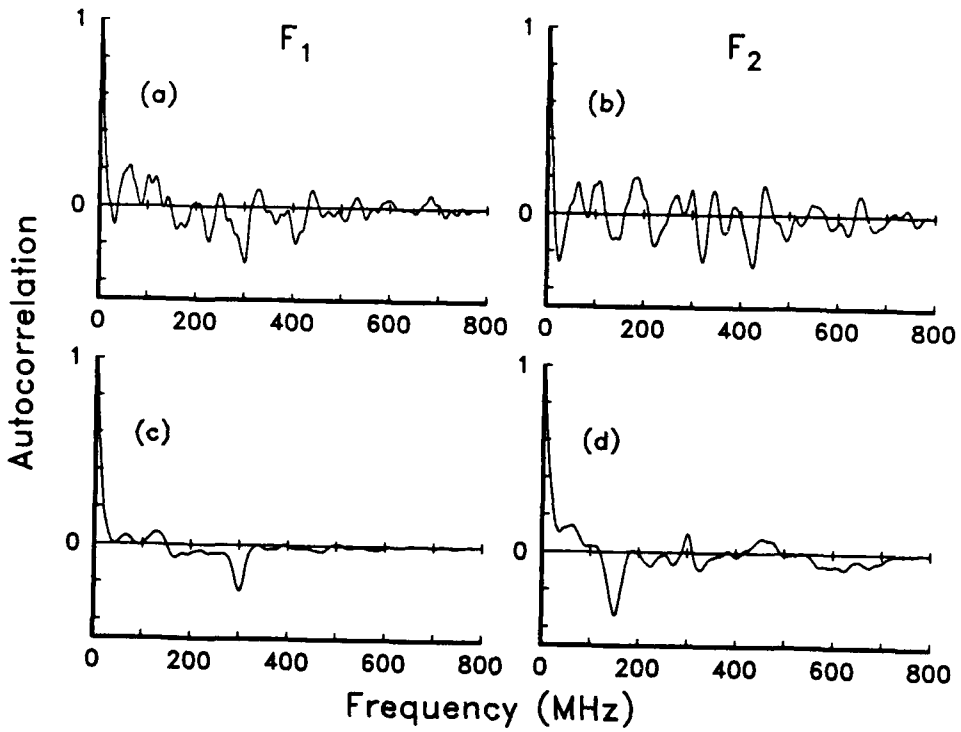
Autocorrelation
1
0
F_1
(a)
F_2
(b)
(c)
(d)
0
200
400
600
800
Frequency (MHz)

Figure 6

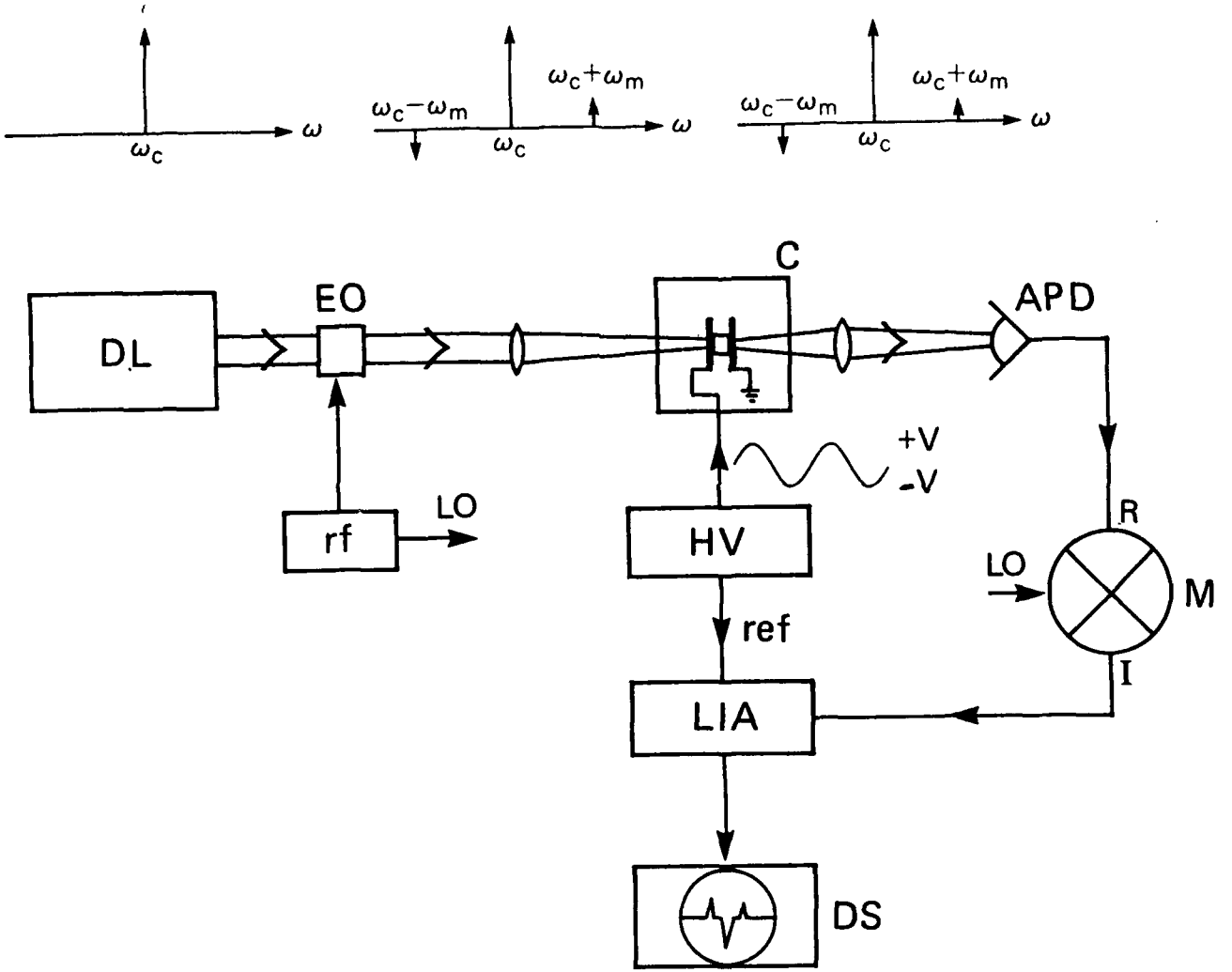
ω_c
ω
$\omega_c-\omega_m$
$\omega_c+\omega_m$
ω_c
ω
$\omega_c-\omega_m$
$\omega_c+\omega_m$
ω_c
ω
C
DL
EO
APD
+V
-V
rf
LO
HV
R
LO
M
ref
I
LIA
DS

Figure 7

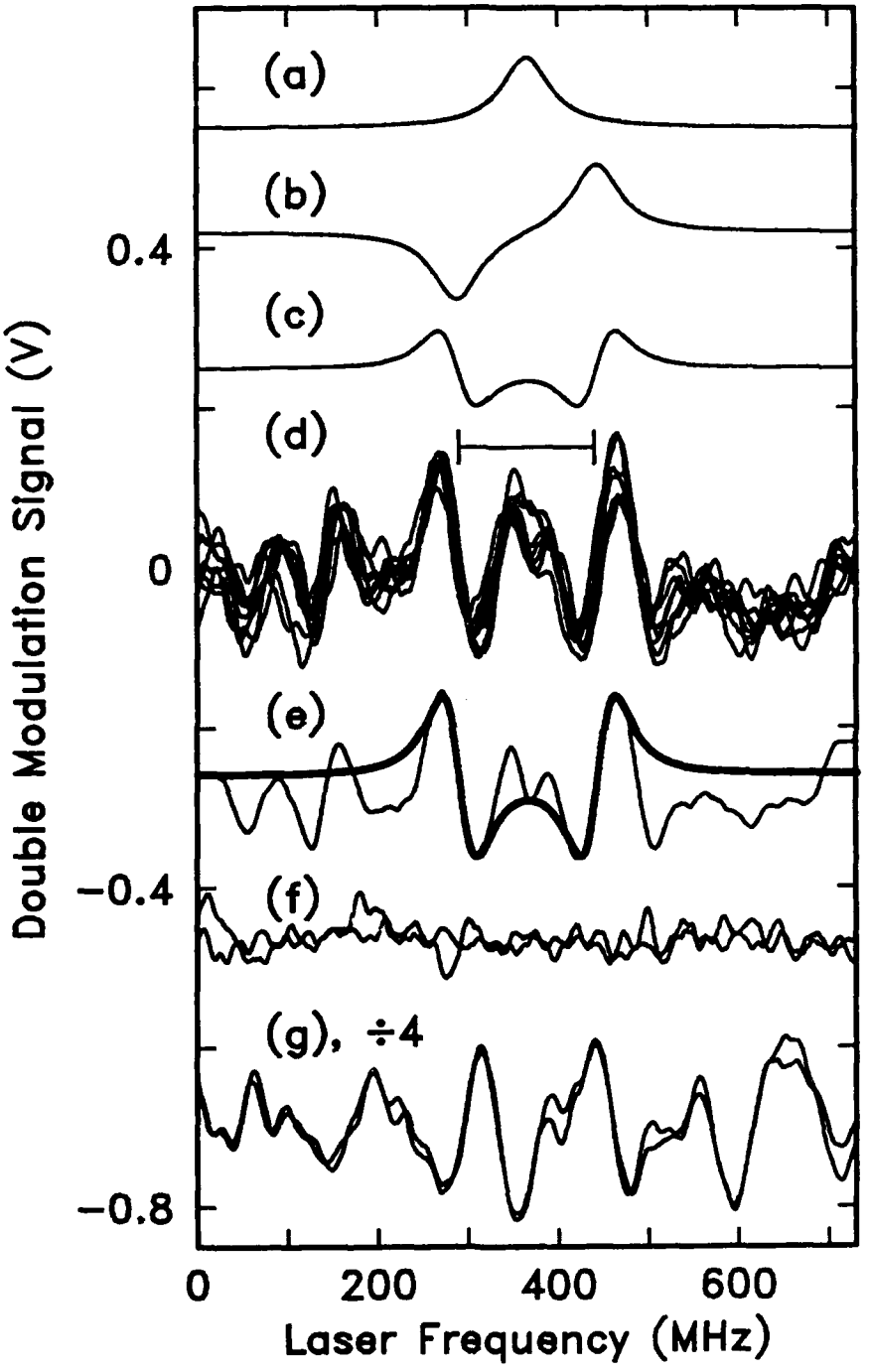
(a)
(b)
(c)
(d)
(e)
(f)
(g), ÷4
0.4
0
−0.4
−0.8
Double Modulation Signal (V)
0
200
400
600
Laser Frequency (MHz)

Figure 8

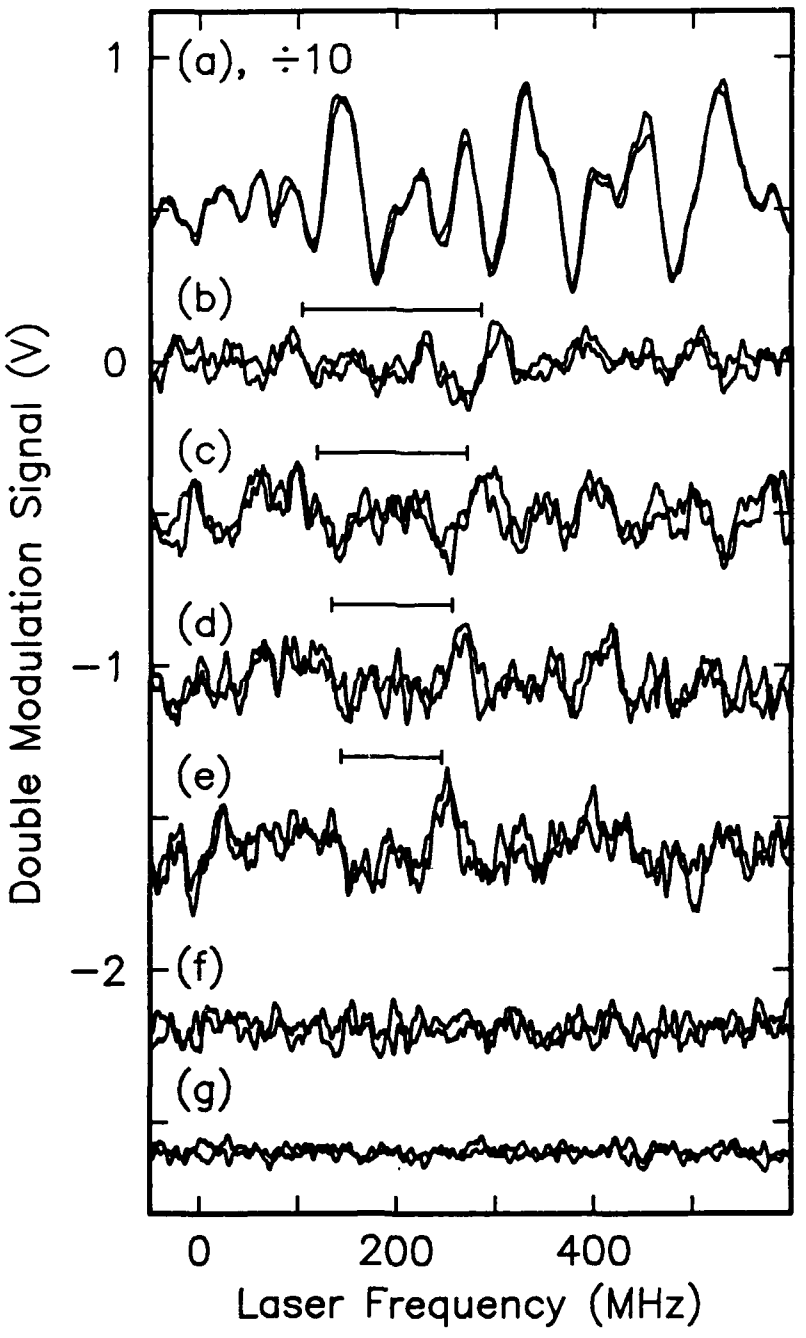
1
(a), ÷10
(b)
0
(c)
(d)
−1
(e)
−2
(f)
(g)
Double Modulation Signal (V)
0
200
400
Laser Frequency (MHz)

Figure 9

TECHNICAL REPORT DISTRIBUTION LIST - GENERAL

Office of Naval Research (2)
Chemistry Division, Code 1113
800 North Quincy Street
Arlington, Virginia 22217-5000

Dr. Robert Green, Director (1)
Chemistry Division, Code 385
Naval Weapons Center
China Lake, CA 93555-6001

Commanding Officer (1)
Naval Weapons Support Center
Dr. Bernard E. Douda
Crane, Indiana 47522-5050

Chief of Naval Research (1)
Special Assistant for Marine Corps Matters
Code 00MC
800 North Quincy Street
Arlington, VA 22217-5000

Dr. Richard W. Drisko (1)
Naval Civil Engineering Laboratory
Code L52
Port Hueneme, CA 93043

Dr. Bernadette Eichinger (1)
Naval Ship Systems Engineering Station
Code 053
Philadelphia Naval Base
Philadelphia, PA 19112

David Taylor Research Center (1)
Dr. Eugene C. Fischer
Annapolis, MD 21402-5067

Dr. Sachio Yamamoto (1)
Naval Ocean Systems Center
Code 52
San Diego, CA 92152-5000

Dr. James S. Murday (1)
Chemistry Division, Code 6100
Naval Research Laboratory
Washington, D.C. 20375-5000

Dr. Harold H. Singerman (1)
David Taylor Research Center
Code 283
Annapolis, MD 21402-5067

ENCLOSURE(2)